# The Role of the Upper Geosphere in Mitigating $CO_2$ Surface Releases in Wellbore Leakage Scenarios

Original Study Prepared for:

**Natural Resources Canada**
**CANMET Energy Technology Centre – Devon**

Prepared by:

ECOMatters


Authors of Poster Session:

Dennis M. LeNeveu
Frank B. Walton
John C. Tait
Marsha I. Sheppard
Kristine Haug, AGS-AEUB

# Introduction

Coalbeds in the Alberta Basin are being investigated both as potential sites for enhanced coalbed methane recovery (ECBM) and for the long-term storage of $CO_2$ and flue gas. Carbon dioxide has a higher affinity for sorption onto coal than methane and can be used to displace the methane during methane recovery operations (Gunter, 2004). After completion of methane resource extraction the coalbeds are candidates for long term storage of $CO_2$.

While numeric reservoir models are used to assess movement of fluids within the coalbeds, more computationally efficient models are required to make a long term, assessment of the impact of potential $CO_2$ leakage into the surrounding geosphere from the proposed coalbed storage formations. CQUESTRA-2 (CQ-2), a semi-analytical model, has been developed to fulfill this latter role. The CQ-2 code assesses the ability of the geosphere to dissolve carbon dioxide from the reservoir and from leaking wellbores (Walton et al., 2004). The spatial extent of the dissolved plume of $CO_2$ as a function of time is determined in each formation allowing for the assessment of the potential impact on human activities of $CO_2$ leakage.

In Part 1 of a two-year project, representative models of the Mannville and Ardley coalbed areas have been developed in cooperation with the Alberta Geological Survey, Alberta Energy and Utility Board (AGS-AEUB). The Mannville coals are relatively deep with a caprock and several thick shale layers acting as barriers to fluid flow from the coal to the surface. The Ardley coals are shallow with few lithological barriers between the coal and shallow potable groundwaters and the surface. Because the Mannville area is likely a more suitable site due to the extensive lithological barriers, only the results from the Mannville study area are reported here. A cartoon illustrating storage of $CO_2$ in the Manville study area is shown in Figure 1.

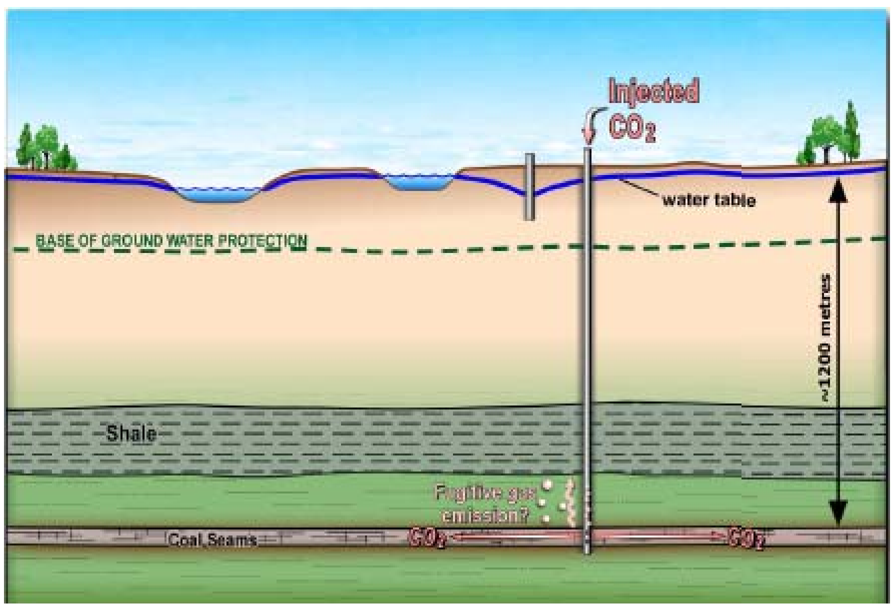


Deterministic modelling studies were undertaken to systematically explore the relationships between well-seal degradation scenarios and the ability of the geosphere above the $CO_2$ storage formation to mitigate potential leakage of $CO_2$ to the biosphere. The ability to estimate both vertical and horizontal distributions of dissolved $CO_2$ within upper geosphere formations is demonstrated.

**Figure 1**

# CQ-2 Model

## Main assumptions:

- The model start time is set after all injection and resource recovery operations have ceased and after the pressure and temperature-transients incurred during injection and resource recovery operations have largely dissipated.
- The start time is long enough for free phase $CO_2$ to form a relatively stable and spatially localized pool in a reservoir under a restraining formation. The free phase would consist mainly of supercritical, gaseous or liquid $CO_2$ mixed with other components such as nitrogen or hydrocarbons. The phase of the mixture would depend on depth and temperature. The restraining formation could be an impermeable caprock, shale layer, coal bed or any other formation that significantly inhibits vertical migration of the free phase $CO_2$. Potential diffusion through this barrier is accounted for in the calculations.
- The potential degradation of the central wellbore plug seal and cement seal in the annular region around the wellbore are modeled as specific failure times for the onset of leakage.

## Model processes:

.

- Potential failure of conventional wellbore seals located in the horizon of the reservoir
- Corrosion of the wellbore casing
- Dissolution of the $CO_2$
- Movement of the free phase into the annular space around the wellbore through degraded cement seals
- Vertical migration of the free phase toward the surface through the annulus and the wellbore
- Transport of the dissolved free phase into the formations surrounding the wellbore and between the reservoir and the surface.
- Mineralization between dissolved $CO_2$ and rock - through the use of a first-order mineralization rate constant

**Figure 2**

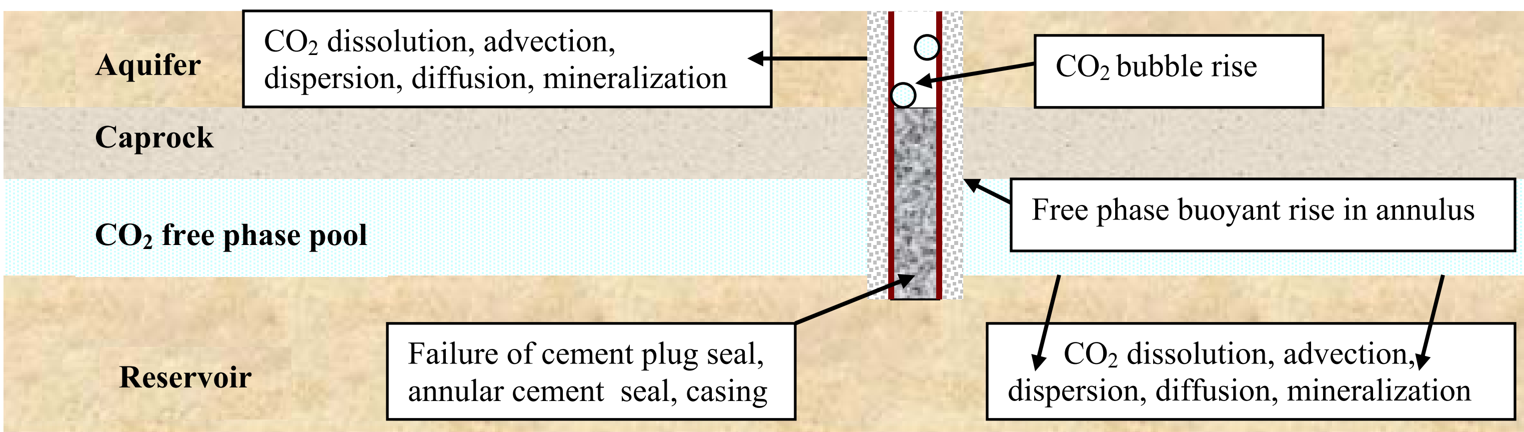

## Model geometry:

- The geological sequestration system is treated as a series of horizontal layers beginning below the restraining formation and extending to the surface. Each layer is determined by the local geological stratigraphy and can be subdivided to increase model discretization.
- The reservoir free phase $CO_2$ is treated as an immobile pool of constant area and diminishing thickness.

## Input Parameters:

The input parameters for the code are straight forward and relatively simple and easy to input through a formatted spreadsheet. The input can be divided into four main groups, formation data, formation fluid data, free phase data and wellbore data. The main data inputs are illustrated in Table 1.

| Formation | Formation Fluid | Free Phase | Wellbore |
|---|---|---|---|
| Depth | Salinity | Mass | Cement seal failure times |
| Thickness | Pressure | Component mole fractions | Casing failure times |
| Reservoir intrinsic permeability | Surface tension with free phase | Relative permeability | Intrinsic permeability degraded cement |
| Porosity | Temperature gradient | Effective saturation | Effective crack diameter degraded cement |
| Tortuosity | Darcy velocity | Critical temperatures | Surface density |
| $CO_2$ mineralization rate | Capillary pressure in reservoir | Acentricity factors | Wellbore dimensions |
| | Dispersion coefficients | Compressibility factors | Relative permeability degraded cement |
| | | Critical pressures | |

**Table 1**

## Calculated parameters:

- Formation fluid density and pore fluid diffusion coefficient for dissolved $CO_2$ are calculated from layer properties to form an internally consistent set of values.
- Free phase properties such as density, viscosity, and solubility are determined from equations of state using algorithms by Duan et al. (2006), Kestin et al. (1985), Guo et al. (2001).
- The density of formation water at various depths and temperature is determined from algorithms from Bachu and Adams (2003).

## Model Output:

- Plumes of dissolved $CO_2$ are tracked in every formation from the reservoir to the biosphere.
- Consequence parameters such as $CO_2$ leakage rates to the biosphere, the sequestered mass in all formations and the mass of the free phase in the reservoir are determined as a function of time.

# Wellbore Component Failure

## Wellbore components:

- steel casing
- cement-filled annulus that provides a seal between the casing and the surrounding rock formation
- cement plug providing an 8-m long seal within the bottom of the casing

## The Four component failure scenarios considered:

- *Failure of the cement plug only*. This is a worst case scenario since an intact casing prevents any mitigation of $CO_2$ releases to the surface by the surrounding aquifer systems. The maximum flow up the well in this scenario is ultimately controlled by the permeability of the host formation, which controls flow to the wellbore.
- *Failure of the cement annulus only*. In this scenario, the vertically migrating $CO_2$ can dissolve into the water within the surrounding formations but the intact casing prevents mass transfer into the well.
- *Failure of the cement annulus and casing*. In this scenario, the vertically migrating $CO_2$ can dissolve into the water within the surrounding formations and into the water within the well casing.
- *Failure of all components*. In this scenario, $CO_2$ dissolved in the water within the casing can undergo mass transfer through the casing and the cement annulus to the surrounding geosphere.

The cement seals can degrade by chemical action or by fracturing, which increases the effective permeability of the cement. The seal between the cement and the casing and between the annulus and the surrounding formations can also degrade or be faulty at the time of cement emplacement. The approach used in this study is to lump their combined effect into a single parameter, the *effective permeability* of the degraded cement which is specified by the user.

Figure 3 shows Potential leakage pathways along an exiting well: between cement and casing (paths a and b), through the cement (c), through the casing (d), through fractures (e), and between cement and formation (f). (taken from Celia et al, 2004)

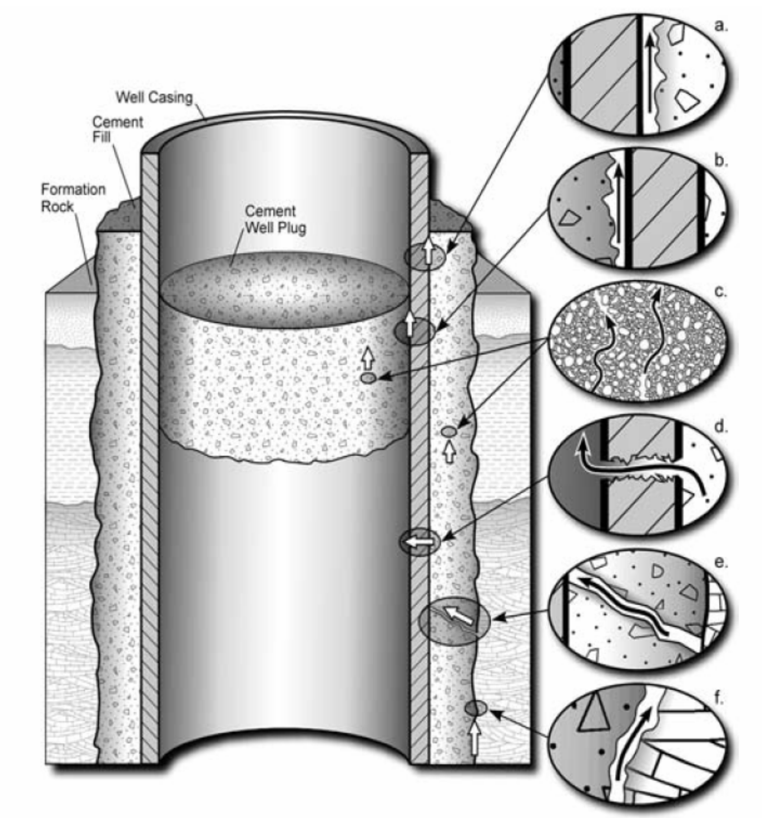


**Figure 3**

# Mannville Study Area

The study area chosen to represent the Mannville coal includes Ft. Assiniboine and is 130 km northwest of Edmonton. The majority of the wells in this area are gas producing or abandoned. There are 97 coalbed methane wells in the study area producing from the Mannville coals in the Corbett, Doris and Neerlandia fields. Figure 4 shows a representative vertical stratigraphic section of the Mannville Study Area. The Mannville coalbed (not shown) is located immediately below the Upper Mannville Aquifer.

## Sequestration Features:

- It was conservatively assumed that mobile $CO_2$ injected into the coal has pooled under the Joli Fou Aquitard.
- The Viking, Badheart, Belly River and Wapiti aquifer systems have the ability to dissolve $CO_2$ before it reaches the surface.
- The dissolution and mineralization of $CO_2$ from the reservoir into the Joli Fou above or the Mannville below was deliberately suppressed.

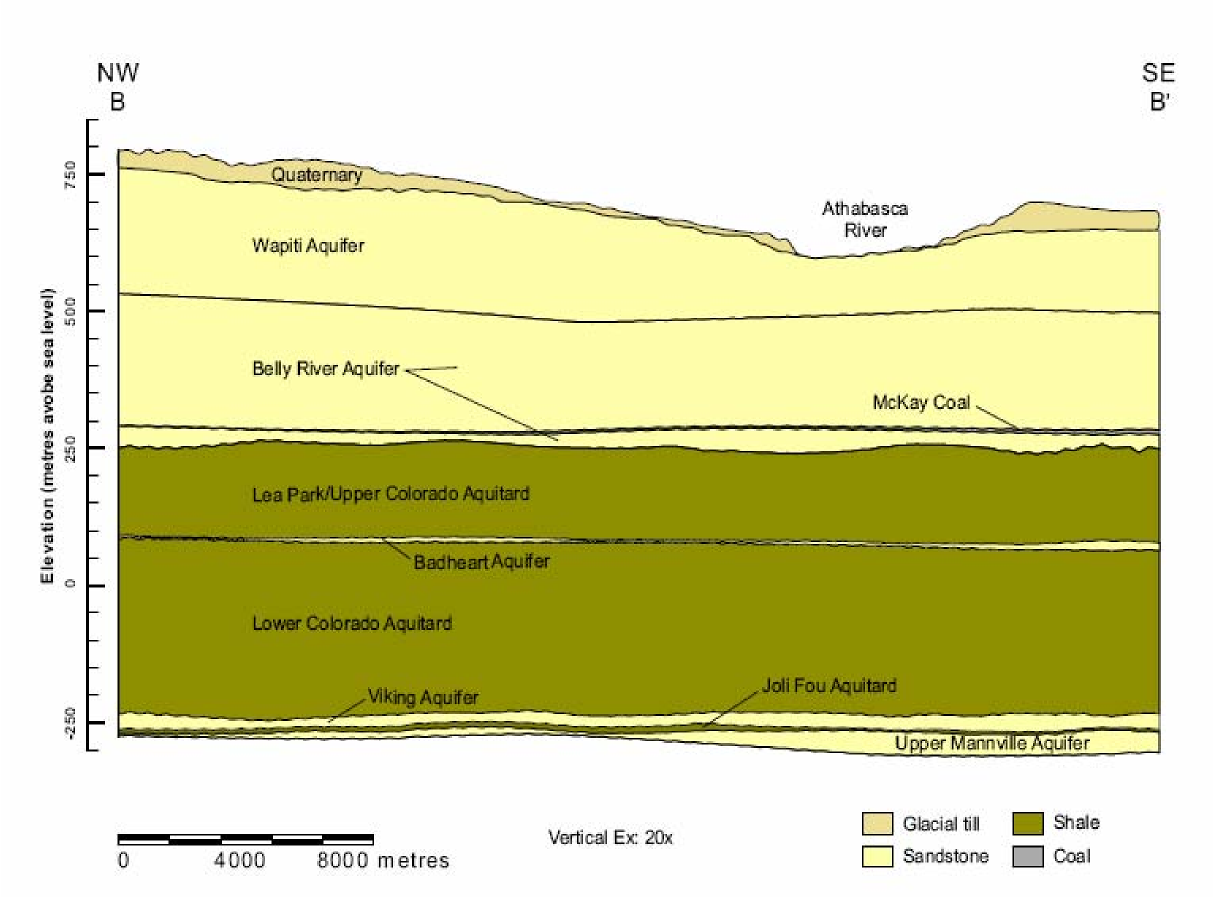


## Data:

The data used to model the Mannville reservoir and upper formations was supplied by the AGS-AEUB (Haug, 2006). In some formations, there were no characterization data. In these cases, data were either estimated or derived.

## Model Geometry:

The stratigraphy of the study area was idealized as a series of horizontal layers. To provide higher vertical resolution of the amount sequestered in the nine formations above the Joli Fou Aquitard (caprock). This part of the geosphere was divided into a total of 27 sub-layers. Formations were divided into sub-layers of equal thickness. The sequence of layers used for the model discretization is illustrated in Figure 9.

**Figure 4**

## Results and Discussion

The four wellbore component failure scenarios described above were investigated. The effective permeability of the degraded cement components was varied from 1 x $10^{-16}$ $m^2$ to 1 x $10^{-12}$ $m^2$. The flow rate into the well components, the amount of $CO_2$ sequestered in the formations above the reservoir and any releases to the surface were calculated. The maximum annual well leakage rates were calculated to be of the order of about $10^{-4}$ of the starting inventory ($10^8$ kg) of the free phase $CO_2$. The calculated flow rates into the well were nearly constant over the first 1000 years.

### Flow rate into wellbore as a function of effective cement permeability:

Figure 5 shows the flow rate into the annulus or plug as a function of the effective permeability of the cement (i.e., casing remains intact). The flow rate into the well components increases linearly as a function of effective cement permeability until it reaches a plateau. At this point, the flow rate into the well components has reached a level where it is limited by the free phase $CO_2$ flow rate within the Mannville Aquifer – the latter being determined by the permeability of the Mannville Aquifer sandstone (geometric mean of $5.67 \times 10^{-14}$ $m^2$). Since the cross-sectional area of the plug is higher than the cross-sectional area of the annulus, the flow rate into the wellbore is proportionately higher than that for the annulus for the same effective cement permeability.

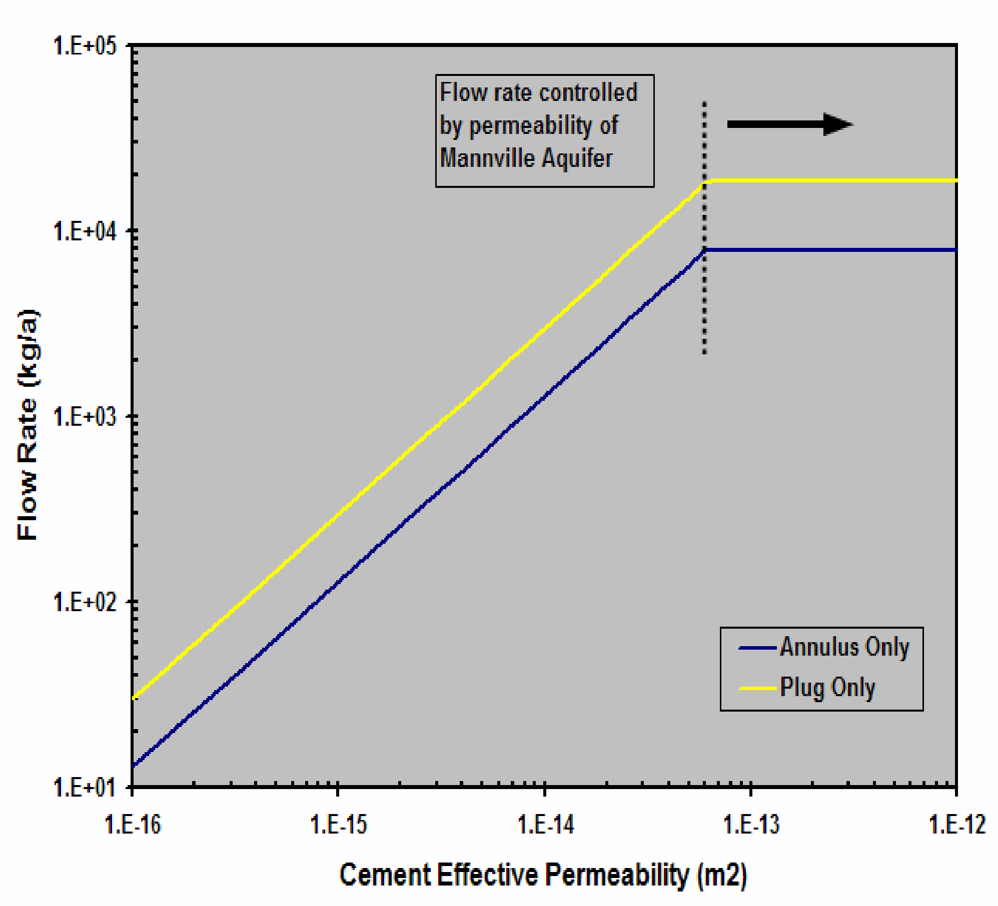


**Figure 5**

**Surface Release Rate for Plug and Annulus, Casing & Plug Failure:**

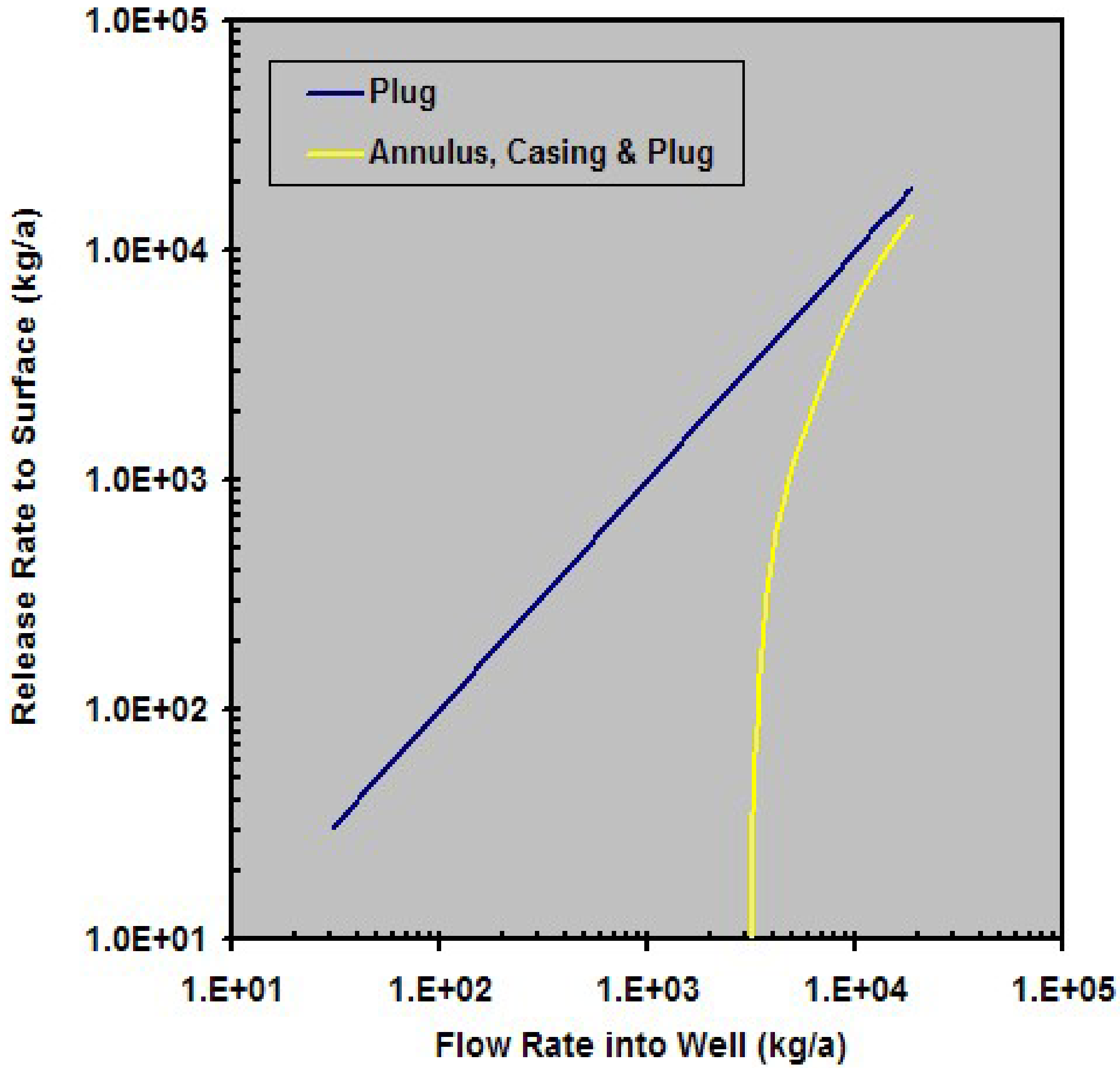


Figure 6 shows surface release rates of $CO_2$ as a function $CO_2$ flow rate into the well components for scenarios where only the plug cement degrades; and, where both the plug and annulus cement degrades, and the casing fails. In the limiting case where only plug cement degrades, the intact casing prevents the interaction of the $CO_2$ with the upper geosphere formations; hence the surface release rate is equal to the flow rate into the well. However, if the casing fails then the $CO_2$ can dissolve in the aquifers above the Joli Fou Aquitard. In this latter case, at well flow rates less than about 3200 kg/a, $CO_2$ surface releases are significantly reduced by sequestration in the upper geosphere.

**Figure 6**

## Surface Release Rate for Annulus and Annulus & Casing Failure:

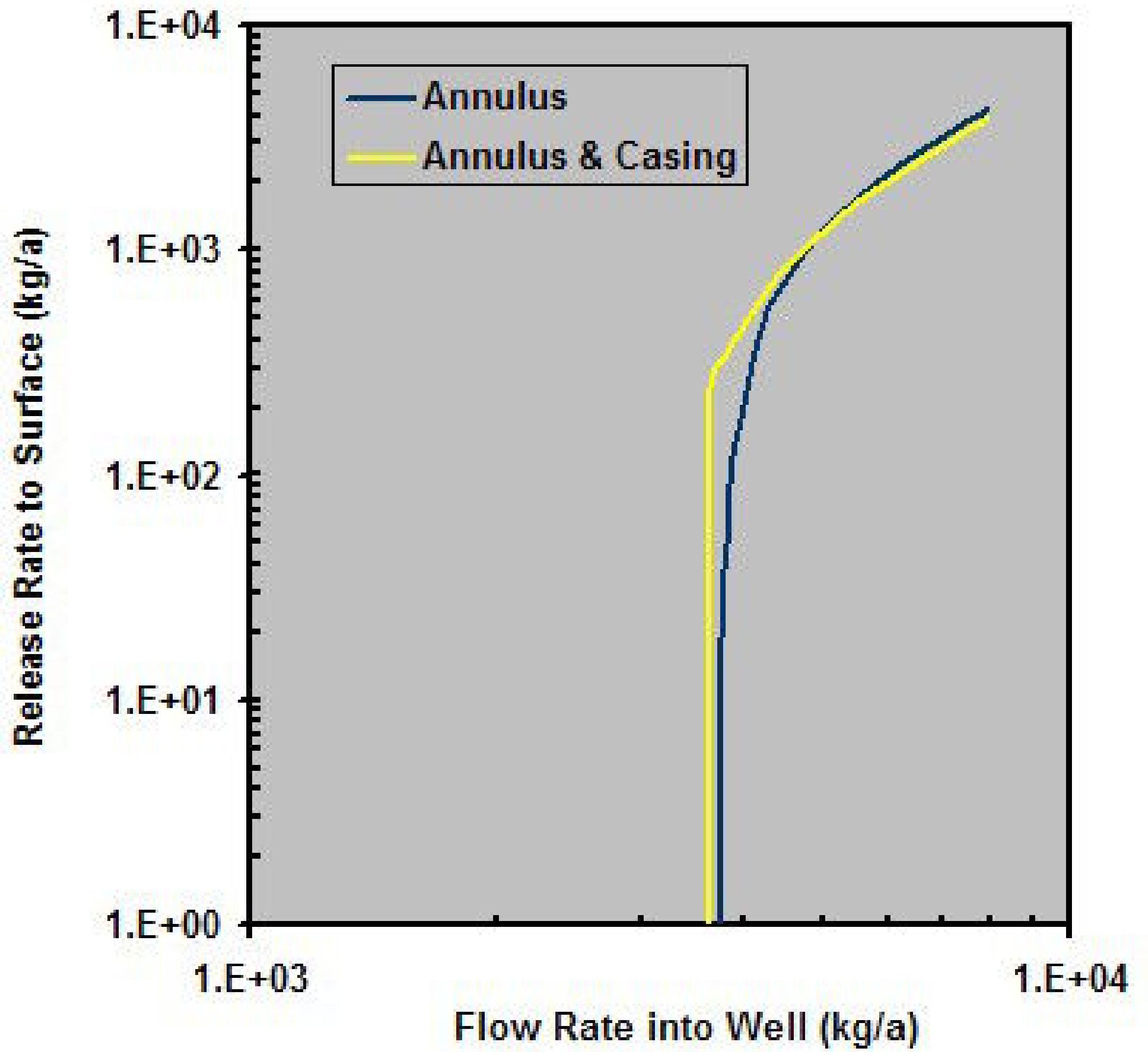


Figure 7 shows surface release rate of $CO_2$ as a function of $CO_2$ flow rate for the two annulus based scenarios. In the case where only the annulus cement degrades there is total sequestration of the $CO_2$ at well flow rates less than about 3750 kg/a. In the case where the casing fails and the annulus cement degrades there is total sequestration at well flow rates less than about 3600 kg/a. This lower flow rate results from the fact that some dissolved $CO_2$ can migrate vertically via the casing cavity thus bypassing any interaction with any surrounding aquifer systems.

**Figure 7**

## Sequestration rate:

In Figure 8 the upper geosphere sequestration rate of $CO_2$ is plotted as a function of $CO_2$ flow rate into well components resulting from three different combinations of component degradation or failure. The CO2 sequestration rate in the upper geosphere formations is equal to the difference between the $CO_2$ flow rate into the well and the $CO_2$ surface release rate. The dashed line defines 100% sequestration of the $CO_2$. The dotted lines define the maximum annulus and plug flow rates as determined by the permeability of the Mannville Aquifer. These latter limits are a function of their respective cross sectional areas – the plug cross section being the greater of the two. In all three scenarios, 100% of the $CO_2$ flowing into the well is sequestered in the upper geosphere for $CO_2$ flows rates ≤3200 kg/a. Flow rates above this level result in leakage to the surface.

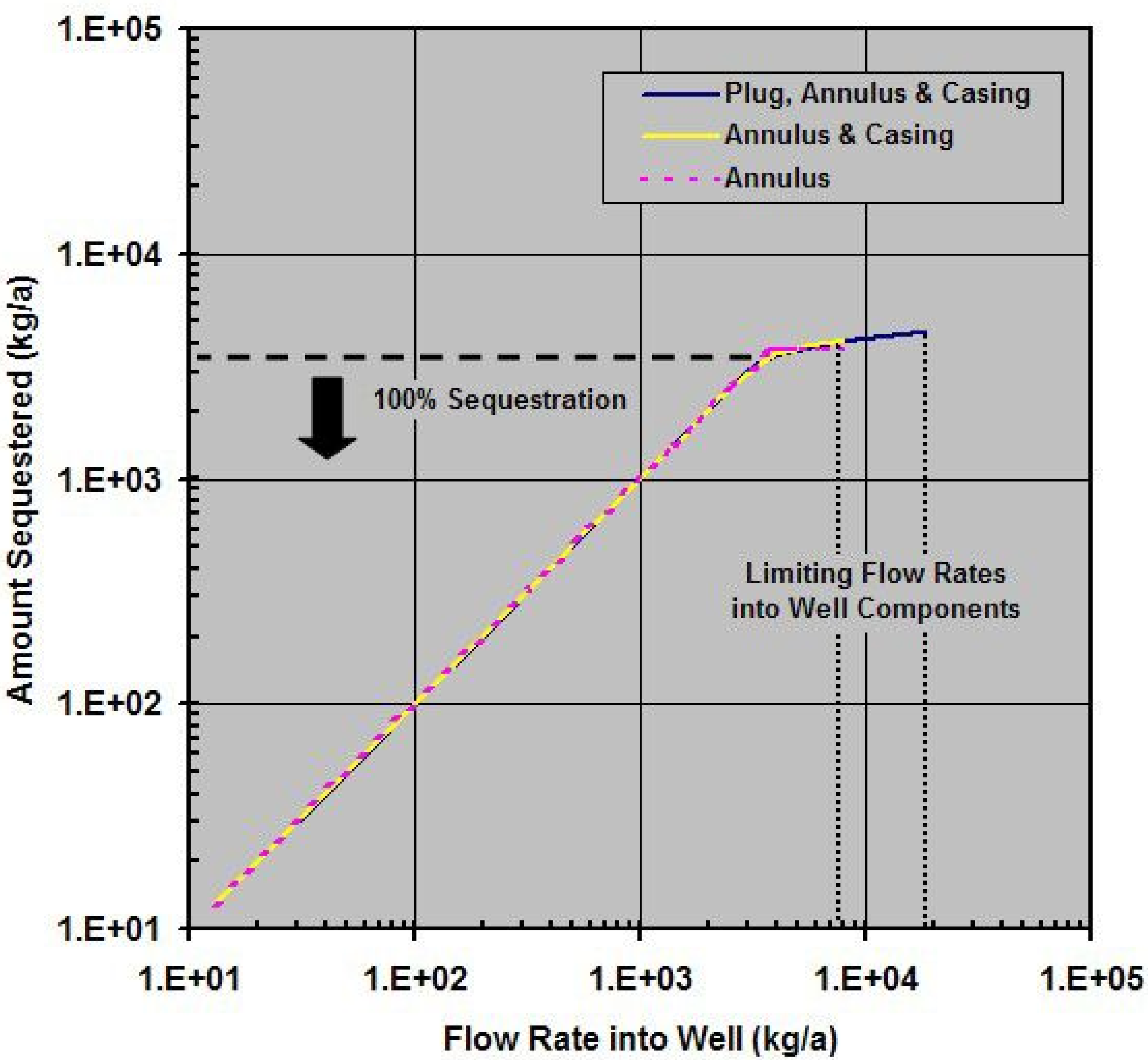


Figure 8

## Amount Sequestered:

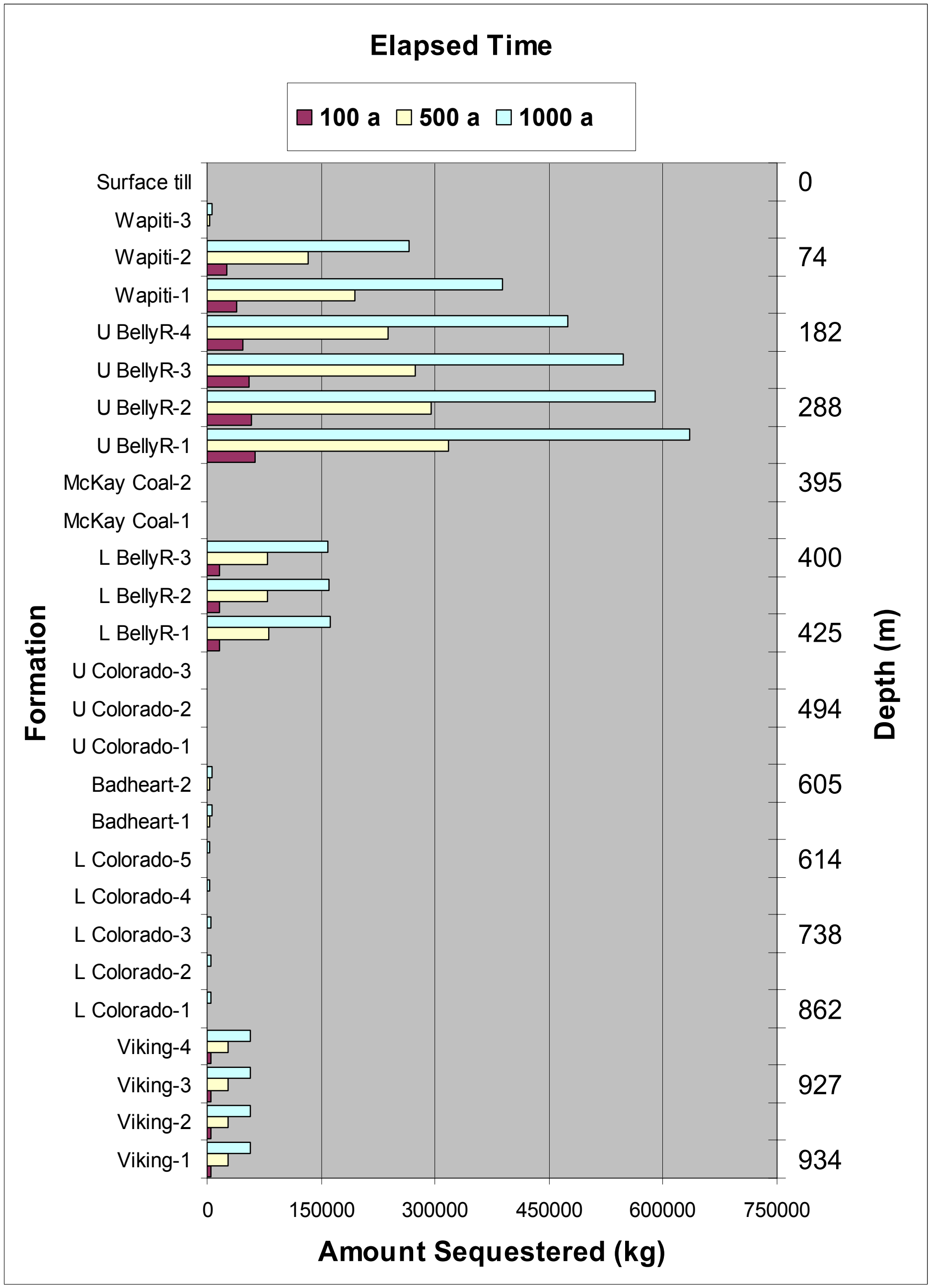


Figure 9 illustrates, for a well flow rate of 3650 kg/a, the cumulative sequestration in each sub-layer for elapsed times of 100, 500 and 1000 years. This latter well flow rate was selected to illustrate how the sequestered $CO_2$ inventory profile with formation depth would look before the well flow rate is large enough to cause surface release of the $CO_2$. The sequestration rate in each sub-layer is proportional to the volumetric flow rate (product of sub-layer thickness, porosity and fluid flow rate) and solubility. Solubility is a function of formation temperature, pressure and salinity. The volumetric flow rate is the dominant factor determining the sequestration rate. The accumulated sequestration inventories in Figure 9 reflect this with the exception of the Wapiti-3 sub-layer. In this case, the well flow rate is not large enough to provide $CO_2$ to this sub-layer because all the $CO_2$ is sequestered by the layers below. The bar chart in Figure 9 also illustrates the model layer discretization used.

Base case estimates indicate that at full sequestration capacity the upper Mannville study area formations can accommodate about 3750 kg/a of dissolved $CO_2$ per wellbore. Of this latter rate the aquifers account for 99.3% and the aquitards only 0.7%, which can only sequester $CO_2$ by diffusion processes.

**Figure 9**

## Sequestration Capacity:

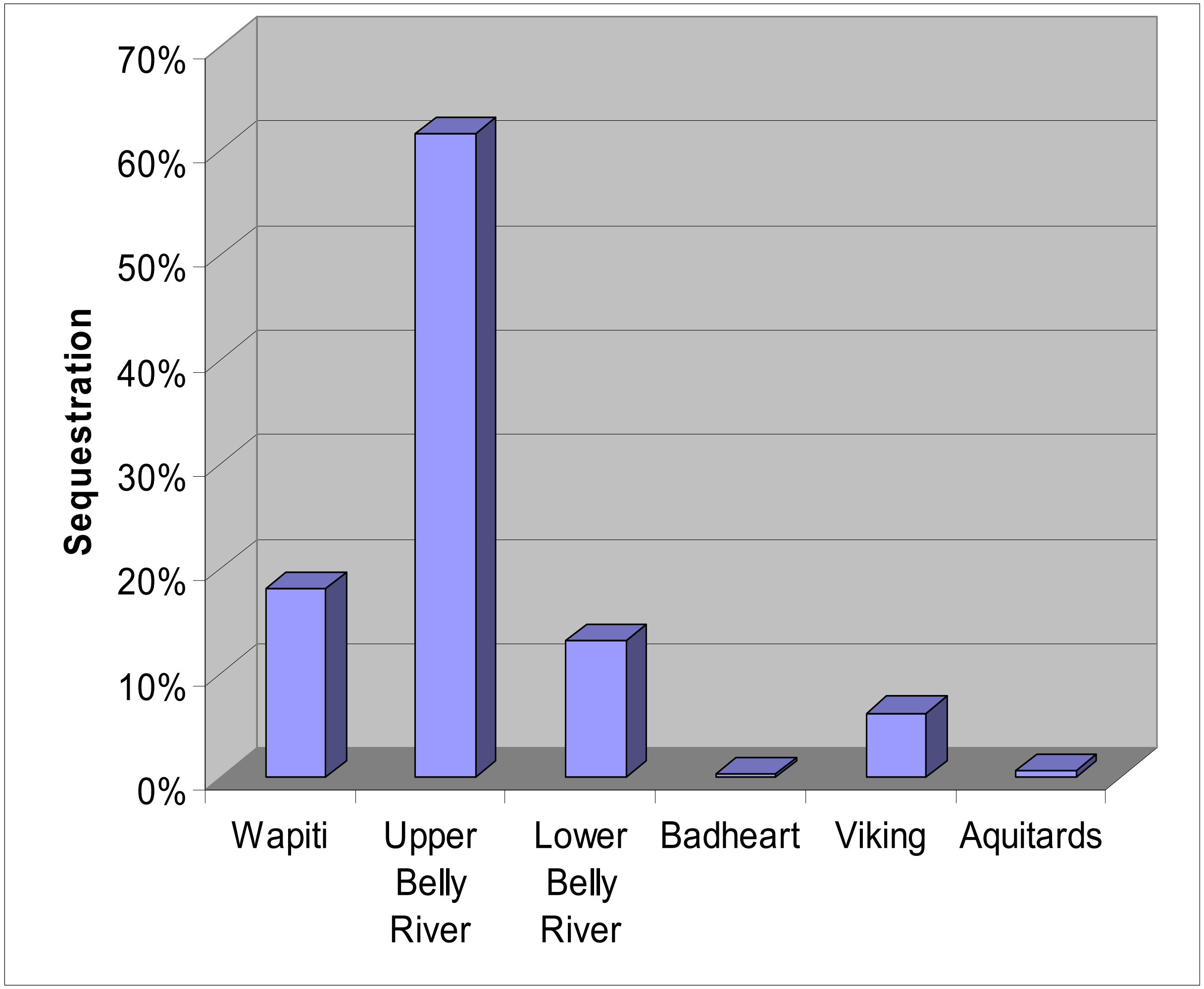


The aquifers listed in Figure 10 represent a total of 99.3% of the total sequestration capacity while the aquitards only contribute 0.7% of the total.

Assuming that the cement in the annulus has degraded to the point where the permeability in the Mannville Aquifer (the host formation) controls the flow, the limiting flow rate into the annulus is about 7930 kg/a. In this scenario, the maximum sequestration rate of 3750 kg/a reduces the flow to the surface by about 45%. In the more extreme scenario, where all wellbore components have degraded or failed, the limiting flow rate controlled by the permeability in the Mannville Aquifer is about 18500 kg/a. In this scenario the sequestration rate reduces the flow to the surface by about 17%. Clearly, the choice of the host formation and/or the choice of the permeability of the Mannville sandstone will have a significant impact on assessing the relative impact of the sequestration capacity of the upper Mannville study area formations on the potential for wellbore related surface leakage of $CO_2$.

**Figure 10**

## Plume Migration of Dissolved $CO_2$ :

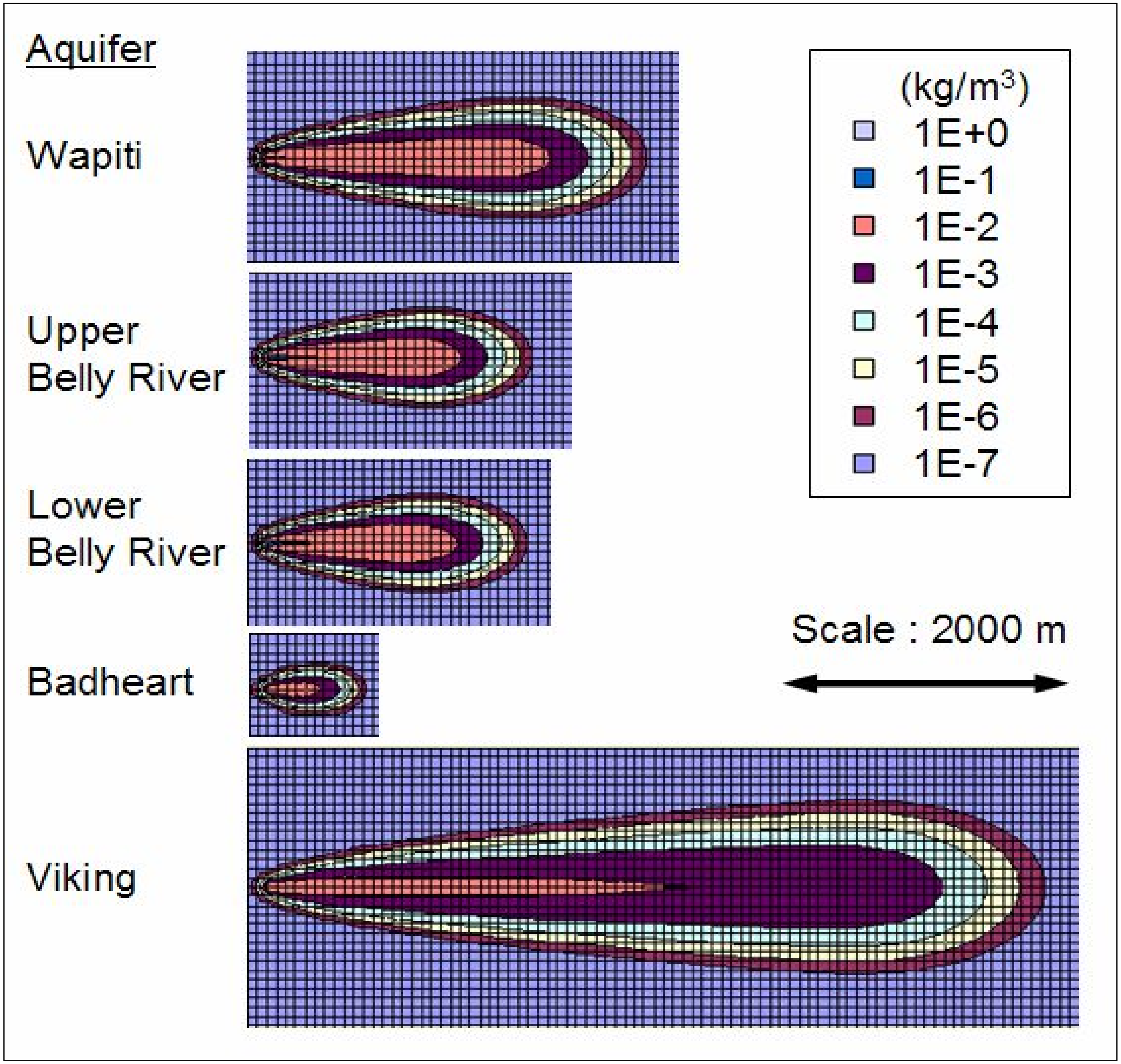


CQ-2 has the ability to provide dissolved concentration gradient profiles for any of the formation layers (or sub-layers) at any point in the elapsed modelling time sequence. This feature helps to visualize the trajectory of the dissolved $CO_2$ plume as it is carried in the aquifer. The calculated $CO_2$ concentrations are available for future chemical reaction studies. Concentration plumes of dissolved $CO_2$ for the aquifers in the Mannville study area at an elapsed time of 1000 years and a $CO_2$ well flow rate of 3700 kg/a. are illustrated in Figure 11. Horizontal and longitudinal distance scales are identical. The spread of the plume parallel to the direction of flow (left to right) reflects the Darcy velocity in the aquifer. Plumes have been aligned in this figure for display purposes only. Groundwater flow directions and rates are documented in the report by Haug, 2006.

**Figure 11**

# Observations & Conclusions

Four well-component degradation scenarios were used in this study to illustrate the impact of various combinations of component degradation or failure.  The issues and conclusions reached in this deterministic study can be summarized as follows:

- If it is assumed that the 8-m long, wellbore cement plug degrades and the steel casing remains intact, then there is direct flow of $CO_2$ up the water-filled well casing to the surface with no possibility for the aquifers above the storage formation to mitigate $CO_2$ leakage.  This combination of well-component performance represents a worst-case scenario.
- All other combinations of well-component degradation and/or failure investigated in this study include some degree of dissolution of the vertically migrating free-phase $CO_2$ into the groundwater and its subsequent advective transport away from the well annulus into the surrounding aquifer systems.  This latter transport rate can be shown to be proportional to an aquifer system's volumetric flow capacity (i.e., product of formation thickness, groundwater flow velocity and porosity) and $CO_2$ solubility.
- .Calculations using base-case geological datasets indicated that the upper Mannville formations have a maximum $CO_2$ sequestration rate of about 3000 kg/a.
- Aquitards located at depths above the $CO_2$ reservoir caprock provide additional physical barriers to the vertical migration of $CO_2$; however, their ability to sequester $CO_2$ resulting from well leakage is limited to diffusion-controlled processes, which represent less than 1% of the amount sequestered in the upper geosphere in these studies.
- In the case of severe cement degradation, $CO_2$ flow-rates into well components eventually become controlled by the permeability of the host formation, which limits the flow rate of $CO_2$ to the well.

The deterministic studies undertaken have provided some general insight into the mechanisms and parameters that affect $CO_2$ sequestration in the upper geosphere of coalbeds and its release to the surface. There is, however, considerable uncertainty associated with many of the present model input parameters for the Mannville system that could be investigated through Probabilistic Risk Assessment in which input parameters are sampled from probability distributions.

# Acknowledgements

Funding for this project is provided through Natural Resources Canada, CANMET Energy Technology Centre – Devon (CETC-Devon) through the Climate Change Technology and Innovation Initiative. The authors gratefully acknowledge the technical oversight and administrative assistance of Dr. Carolyn Preston of NRCan in this project.  The authors would also like to acknowledge the assistance Dr. Stefan Bachu of AGS-AEUB who facilitated setting up the lines of communication between ECOMatters and AGS-AEUB that have resulted in the creation of the Mannville and Ardley geological models.  These latter models make this study of timely relevance to ongoing developments in the area of ECBM recovery and potential flue gas storage within the Alberta coal beds.

## References

Bachu, S. and Adams, J.J. (2003). Sequestration of $CO_2$ in Geological media in Response to Climate change: Capacity of Deep Saline Aquifers to Sequester $CO_2$ in Solution.

Bear, J. (1972). Dynamics of Fluids in Porous Media, Dover Publications, New York.

Celia, M.A., Bachu, S., Nordbotten, J.M., Gasda, S.E. and Dahle, H.K. (2004). Quantitative Estimation of $CO_2$ Leakage from Geological Storage: Analytical Models, Numerical Models, and Data Needs, Proceedings of GHGT-7 Conference, Vancouver B.C, September 2004.

Duan, Z., Sun, R. Zhu C. and Chou, I-M. (2006). An improved model for the calculation of CO2 solubility in aqueous solutions containing Na+, K+, Mg2+, Cl-, and SO42-. Marine Chemistry 98; 131-139

Gunter, W.D, Mathew J. Mavor,M,J, and Robinson, J.R. (2004). $CO_2$ Storage and Enhanced Methane Production: Field Testing at Fenn-Big Valley, Alberta, Canada, with application. Proceedings of 7th International Conference on Greenhouse Gas Control Technologies. Volume 1: Peer-Reviewed Papers and Plenary Presentations, IEA Greenhouse Gas Programme, Cheltenham, UK.

Gunter, W.D., Mavor, M. J. and Robinson, J.R. (2004). $CO_2$ Storage and Enhanced Methane Production: Field Testing at Fen-Big Valley, Alberta, Canada, with Application, GHGT-7 Conference, Vancouver B.C., September 2004.

Guo, X.Q., Sun, C.Y., Rong, S.Y., Chen, G.J. and Guo, T.M. (2001). Equation of state analog correlations for the viscosity and thermal conductivity of hydrocarbons and reservoir fluids. Journal of Petroleum Science and Engineering 30: 15–27.

Haug, K. (2006). Geological and Hydrogeological Characterization of the Sedimentary Succession in Areas Representative of Potential $CO_2$ Storage in Coal Beds in Alberta. Alberta Geological Survey, Alberta Energy and Utilities Board.

Kestin, J., Imaishi, N., Nott, S.H., Nieuwoudt, J. C. and Sengers, J.V. (1985). Viscosity of light and heavy water and their mixtures. Physica A: Statistical and Theoretical Physics, 134☹1): 38-58.

Walton, F.B., Tait, J.C., LeNeveu, D. and Sheppard, M.I. (2004). Geological Storage of $CO_2$: A Statistical Approach to Assessing Performance and Risk. GHGT-7 Conference, Vancouver, B.C., September 2004.